Hindawi
Advances in Materials Science and Engineering
Volume 2019, Article ID 7976580, 12 pages
https://doi.org/10.1155/2019/7976580

*Research Article*

# The Mechanical Properties of a Smart Compression-Type Isolator Based on Magnetorheological Gel and Magnetorheological Elastomer

**Guo-Jun Yu**,[1] **Xi-Xi Wen**,[1] **Cheng-Bin Du**,[2] **and Fei Guo**[3]

[1]*Faculty of Civil Engineering and Mechanics, Jiangsu University, Zhenjiang 212013, Jiangsu, China*
[2]*Department of Engineering Mechanics, Hohai University, Nanjing 210098, China*
[3]*Seazen Holdings Corporation, Shanghai 2000000, China*

Correspondence should be addressed to Guo-Jun Yu; gjyu9@ujs.edu.cn

Received 17 July 2018; Revised 10 December 2018; Accepted 14 January 2019; Published 10 February 2019

Academic Editor: Marco Rossi



In order to control the vibration of civil building structures, a smart extrusion-type isolator was developed based on magnetorheological gel (MRG) and magnetorheological elastomer (MRE). The key technology and performance tests of the isolator were investigated as well as the identification of parameters of the mechanical model. Test results showed that the MRG cylinder has a damping characteristic at high frequency while the MRE cylinder has an isolation characteristic at low frequency. The designed isolator is therefore superior over the traditional isolator since it will show small damping and low dynamic stiffness at a high frequency and small amplitude situation, which can overcome stiffness hardening that occurs on the traditional isolator. Meanwhile, the designed isolator will also have the behavior of large isolation and high dynamic stiffness under the low frequency and large amplitude condition, which has the advantage of realizable displacement control. The uniaxial mechanical model for the MRG/MRE smart isolator was built, and the parameters of the designed vibration isolator were identified. Theoretical results obtained from the mechanical model of the MRG/MRE smart isolator agree well with the experimental results indicating that the parameter identification method is feasible and effective.

## 1. Introduction

Conventional vibration isolation techniques which are often used to reduce the civil structure vibration contain isolation (foundation isolation), transference (vibration absorption), energy dissipation (energy consumption), etc. The isolation effect of these methods is significant for a confirmed vibration; however, it is limited when the characteristic of vibration excitation or dynamic characteristic of the structure changes. Therefore, more and more attention has been paid currently to active shock damping technology, which also has limited application yet due to some drawbacks such as its complexity, high price, and large energy consumption. Hence, many other researchers have been devoted to study semiactive vibration isolation technology (i.e., adjustable damping and/or stiffness) because of its simple structure, low cost, and small energy consumption [1–5]. The family of MR materials has been proposed to achieve variable stiffness and damping for decades, among which MRE and MRG have been used widely by researchers to semiactive isolation systems because they both help intrinsically to solve the distinct problem such as a mismatch of the particles of magnetorheological fluid (MRF) [6–11].

In the past decade, most of the research studies have focused on the magnetic-field-induced shear property of MRE while limited on compression property because of the lack of good computational models. However, polymer-based materials can bear more loads in compression status than in shear status, and most of them often work in compression status. Liao et al. [12] studied the magnetic-field-induced normal force of MRE under compression status both experimentally and theoretically. They found that the magnetic-field-induced normal force increases with increasing magnetic field and increasing precompression

force. Fu et al. [13] designed a new MRE isolator in the shear-compression mixed mode. They utilized two pieces of MRE fabricated with different dimensions in the isolator. The results showed that the natural frequency of the MRE isolator changes greatly with variable current applied, and the amplitude of vibration is attenuated widely. Compared with the natural frequency of 0 A, the increment of the natural frequency is up to 103% with applied current reaches to 1.5 A. Jie et al. [14] developed a magnetorheological elastomer isolator with the shear-compression mixed mode. Experiments showed that the resonance frequency of the MRE isolation system shifted from 45.82 Hz (0 A) to 82.55 Hz (1.5 A). Meanwhile, the relative change in equivalent stiffness and damping was 175% and 216%, respectively, and the relative change in the isolator force was 190% from 0 A to 1.5 A.

MRG is analogous to MRF and MRE. MRG contains micron-sized magnetic elements such as CI or iron particles, and these magnetic elements are dispersed into the grease. Many researchers have prepared variable MRG and tested their rheological property [9, 15, 16]. Like MRF, MRG can also be used in developing linear and disk-type MR damper, which solves the sedimentation problem existing in MRF. Sugiyama et al. [17] developed a new type of controllable working fluid using grease as the career of magnetic particles, and they introduced them into a cylindrical damper and tested its performance. It was shown that the MR grease damper worked effectively as a semiactive damper. Shiraishi and Misaki [18] developed a controllable shear type damper using the MRG, and its performance was experimentally verified. It is confirmed that MRG has the high dispersion stability, and the semiactive vibration control is successfully conducted by the MR grease damper using the control algorithm.

Some researchers have developed both stiffness and damping variable devices which are more effective than only stiffness or only damping devices. Sun et al. [19] designed and manufactured an isolator whose damping and stiffness can be simultaneously controlled by MRF and MRE. They also designed stiffness and damping variable damper through the compact assembly of two MRF damping units and a spring [20]. Greiner-Petter et al. [21] designed a device by utilizing two magnetorheological fluid valves and two springs. However, MRF exhibits variable problems such as particle settlement and poor sealing. Thus, MRG and MRE are utilized in the paper to overcome the above defects and achieve the effect of variable stiffness and damping. The paper is presented by the following orders. Section 2 prepared MR materials used in the designed isolator. Section 3 showed a detail structure of the MRG/MRE isolator and its working principle. Section 4 presented magnetic circuit design of the isolator. Section 5 tested the performance of the isolator. Section 6 built the mechanical model of the isolator and identified the parameters. Section 7 contains the conclusion.

## 2. Materials Preparation and Testing

In the present experiments, carbonyl iron (CI) particles with a mean particle size of 3.5 $\mu$m were used as the magnetic particles; gelatin, agaropectin, polydimethylsiloxane (PDMS), and glycerol were used as the matrix materials of MRGs; polyethylene glycol (PEG-400) and oleic acid were used as the surfactants of soft magnetic particles; and the absolute ethyl alcohol was used as the dispersant of MRGs. Besides, polyurethane (PU) rubbers were chosen as the matrix of MREs; dicumyl peroxide (DCP) and dioctyl phthalate (DOP) were, respectively, used as a sulfurizing reagent and plasticizer. All the reagents are of analytical purity and purchased from Sinopharm Chemical Reagent Co., Ltd. in China.

MRG is a gelatinous suspension system in which the soft magnetic particles are dispersed in the carriers. To achieve excellent performance, the soft magnetic particles should be uniformly dispersed in the carriers. In this work, MRGs were prepared by uniformly dispersing the soft magnetic particles in the carriers through ball milling progress. Figure 1 shows the specific preparation process of MRG.

On the basis of the aforementioned method, 5 groups of samples marked by MRG-1 to MRG-5 with excellent dispersity in which the soft magnetic particles account for 72% were prepared. Table 1 lists the composition of each MRG sample. The ratio of gelatin to agaropectin is 3 : 1.

MRE is a kind of viscoelastic material which is formed by dispersing micron-sized soft magnetic particles in viscoplastic high-molecular polymer matrix and cured under a magnetic field with certain intensity.

The preparation of MRE consists of three major steps: mixing, preconfiguration, and sulfuration. In this work, XK-160 double-roll mill was used to disperse CI particles, dicumyl peroxide DCP, and plasticizer DOP into the PU matrix uniformly. During the preconfiguration stage, the rubber compound was placed in a thermal magnetic coupling system to form chain structures at the condition of magnetic flux density 1 T and 80°C for 15 min. After shutting down the magnetic field, the temperature was raised to 145°C. In this condition, the sample was on sulfuration for 15 min, and the MRE was obtained. The mass fraction of CI particles of the prepared MRE sample is 85%, and other composition of MRE is the same with MRG-5.

The rheological properties of MRG and MRE were tested by MCR302 rotary rheometer. Figure 2(a) shows the shear stress of MRG samples as a function of magnetic flux density. It can be observed that the mass fraction of solution determines the shear yield strength of MRGs. Taking MRG-5 with highest content of solution, for example, the shear yield strength reaches to 92.1 kPa. Figure 2(b) displays the relationship between apparent viscosities of MRG-5 sample and shear rate. MRG exhibits obvious shear thinning phenomenon, and the apparent viscosity increases with increasing magnetic flux density. Furthermore, for MRG-5, when the magnetic field is turned off (zero magnetic field), the initial viscosity is only 11.8 Pa·s.

Figure 3 shows the shear storage modulus of MRE as a function of magnetic flux density at different strains. The shear storage modulus of MRE decreases with increasing strain, which can be called the Payne effect of MRE [16]. It can be seen from Figure 3 that MRE has larger initial shear modulus, but smaller magnetic-field-induced modulus when strain is small; however, smaller initial shear modulus and larger magnetic-field-induced modulus when strain is large.

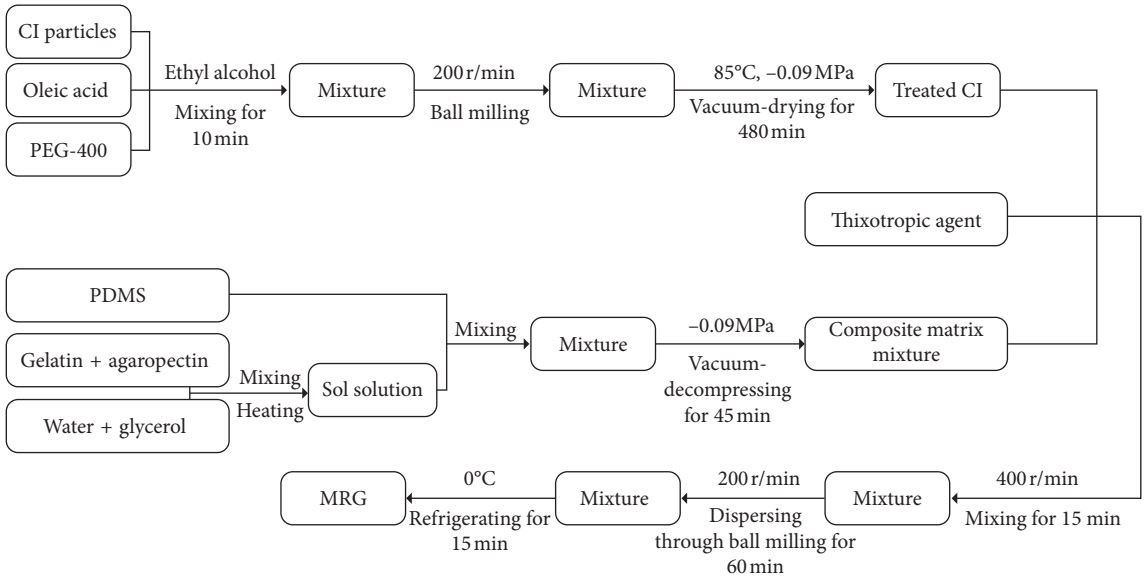


Figure 1: The preparation process of MRG.

Table 1: The composition of MRG samples (mass fraction).

| Samples | CI particles (%) | Matrix-25% | | Thixotropic agent (%) |
|---|---|---|---|---|
| MRG-1 | 72 | PDMS/matrix-100% | Solution/matrix-0% | 3 |
| MRG-2 | 72 | PDMS/matrix-90% | Solution/matrix-10% | 3 |
| MRG-3 | 72 | PDMS/matrix-80% | Solution/matrix-20% | 3 |
| MRG-4 | 72 | PDMS/matrix-70% | Solution/matrix-30% | 3 |
| MRG-5 | 72 | PDMS/matrix-60% | Solution/matrix-40% | 3 |

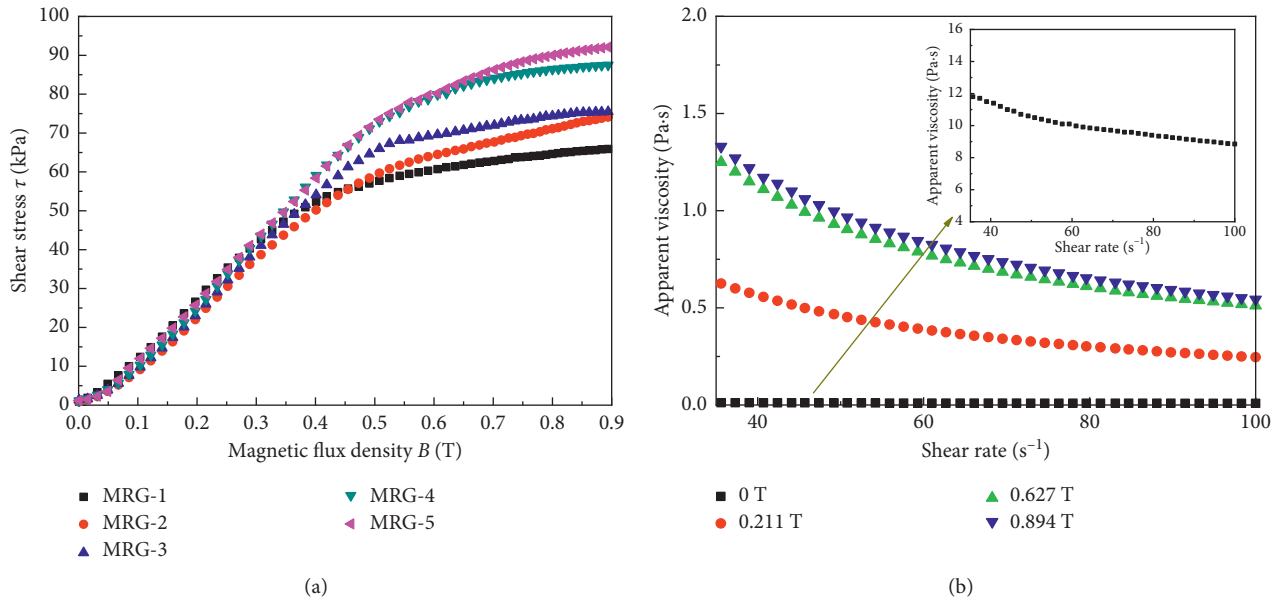


Figure 2: (a) The shear stress stimulated by different magnetic flux density for MRG-1 to MRG-5 and (b) the apparent viscosity of MRG-5 versus shear rate.

The magnetorheological effect of MRE with too large or too small strain will be affected because when MRE has large strain, the distance between internal particles increases, and the magnetic attraction decreases, resulting in the decrease of magnetic-field-induced modulus. The contribution of magnetic particles to the initial storage modulus is too large when strain of MRE is too small, which makes the initial modulus of MRE larger than that with larger strain. Meanwhile, absolute magnetorheological effect (AMRe) and relative magnetorheological effect (RMRe) are introduced in

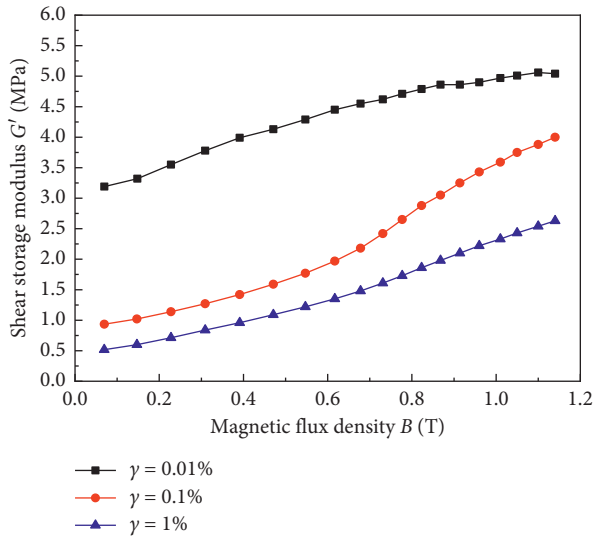


Figure 3: Variation of shear storage modulus with magnetic flux density for MRE at different strains.

Equation (1) to quantify the magnetorheological property. $G'_{max}$ is the maximum storage modulus of MRE induced by the external magnetic field, and $G'_{min}$ is the initial shear storage modulus. Table 2 lists the detailed parameter values at different strains. For example, at strain of 0.1%, AMRe of MRE reaches to 3.0 MPa and the RMRe is 300%. Besides, RMRe of MRE increases with increasing strain:

$$\begin{aligned} \text{AMRe} &= G'_{max} - G'_{min}, \\ \text{RMRe\%} &= \frac{G'_{max} - G'_{min}}{G'_{min}} \times 100\%. \end{aligned} \tag{1}$$

## 3. Design of the MRG/MRE Smart Isolator and Working Principle

The goal of building seismic fortification is "not bad under small earthquake, can be repaired under medium earthquake, cannot collapse under large earthquake." That is to say, when encountering frequent earthquakes (small earthquakes), the building is basically in the elastic stage, only small displacement occurs. Under rare earthquakes, the building is seriously damaged and large displacement occurs but not collapse. According to the "Code for seismic design of buildings GB 50011–2010" of the National Standards of the People's Republic of China, the paper designed a small displacement of 6 mm and a large displacement of 12 mm to achieve the goal of two-level seismic fortification for the isolator aiming at 3.3 m single-storey reinforced concrete frame structure.

In order to achieve these two objectives, the isolator was designed in two stages, using MRG and MRE, respectively, achieving the damping characteristic on high frequency of 6 mm and the isolation characteristic on low frequency of 12 mm.

*3.1. Structural Design.* A schematic of the designed isolator is shown in Figure 4. The biggest difference is that both MRG and MRE are incorporated by this smart isolator. As shown in Figure 1, the isolator includes a MRG cylinder and a MRE cylinder. The MRG cylinder is mainly composed of up-plate, sealing, excitation coil, and working gap filled with MRG. Obviously, like MRF, the operating mode of the MRG cylinder in the isolator is shear mode. The damping of MRG is controllable, depending on magnetic density by introducing different currents into the excitation coil. The MRE cylinder is mainly composed of down-plate, slip ring, excitation coil, and MRE. Similarly, the stiffness of MRE is controllable by changeable current. The most noteworthy in terms of the MRE cylinder is that the operating mode of MRE is compression mode, which can bear more loads in compression status. The material is prepared and the structure is designed, and the most important procedure is to determine the size according to the required force. The output force generated by MRG and MRE cylinder can be calculated by the following equations.

Table 2: Parameters of MRE with external magnetic field at different shear strains.

| Strain (%) | $G'_{max}$ (MPa) | $G'_{min}$ (MPa) | AMRe (MPa) | RMRe (%) |
|---|---|---|---|---|
| 0.01 | 5.040 | 3.190 | 1.850 | 58 |
| 0.1 | 4.000 | 1.000 | 3.000 | 300 |
| 1 | 2.630 | 0.517 | 2.113 | 409 |

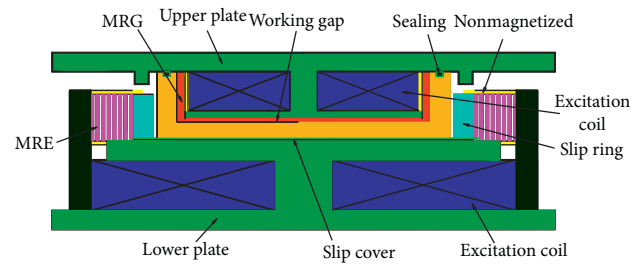


Figure 4: Schematic design of the MRG/MRE smart isolator.

Since the property of MRG is similar to MRF, the damping force of the MRG cylinder can be represented as follows [22]:

$$F_{MRG} = \frac{\eta A_p}{h}\dot{\gamma} + \tau_y A_p \text{sgn}(\dot{\gamma}), \tag{2}$$

where $\eta$ is the dynamic viscosity of MRG; $A_p$ is the effective working area of the MRG piston of a isolator; $h$ is the working space height; $\dot{\gamma}$ is the shear strain rate of MRG; $\tau_y$ is the shear yield strength of MRG.

The force generated by the MRE cylinder can be calculated by the following equation [23]:

$$F_{MRE} = E\frac{DA_r}{T_r} + 48\pi\mu_0\mu_r\frac{a^6}{s^4}H^2(1-\cos\varphi), \tag{3}$$

where $E$ is the compressive elastic modulus of MRE; $E = 5.4GS^2$, where $G$ is the shear elastic modulus of MRE; $S$ is the shape factor of the isolator; $D$ is the level relative displacement between upper and under plate of the isolator; $T_r$ is the total thickness of MRE; $A_r$ is the extrusion area of MRE; $\mu_0$ is the permeability of vacuum ($4\pi \times 10^{-7} H/M$);

$\mu_r$ is the relative permeability of MRE; $a$ is the radius of ferromagnetic particles; $s$ is the center distance between the ferromagnetic particles; $H$ is the external magnetic field strength; $\varphi$ is the radian of the particles chain.

Overall, the force of the designed isolator can be integrated into the following equation:

$$F = \frac{\eta A_p}{h}\dot{\gamma} + \tau_y A_p \operatorname{sgn}(\dot{\gamma}) + \delta\left(E\frac{DA_r}{T_r} + 48\pi\mu_0\mu_r\frac{a^6}{s^4}H^2(1-\cos\varphi)\right), \quad (4)$$

$$\begin{cases} \delta = 0, & |D| \le 6, \\ \delta = 1, & 6 < |D| \le 12. \end{cases}$$

Equation (4) provides the guidelines for the design of size of the MRG/MRE isolator. After repeated adjustment of the design process, the main design parameters of the smart isolator can be confirmed as shown in Table 3.

*3.2. Working Principle.* The designed MRG/MRE smart isolator structure mainly includes a MRG cylinder and a MRE cylinder. For the MRG cylinder, the force is generated mainly by damping force of MRG, which is controllable due to variable damping of MRG under different magnetic field intensities. The shear stress of MRG will be enhanced by increasing the current applied to the excitation coil set on the MRG cylinder, resulting in larger damping force, conversely, smaller force.

For the MRE cylinder, when subjected to heavy loads, it will have greater force by increasing current applied to the excitation coil set on the MRE cylinder. That is because stiffness of MRE increases when magnetic field intensity increases and decreases when magnetic field intensity decreases.

To sum up, in different vibration environments, the stiffness of MRE and damping of MRG can be adjusted by changing the current, so that the intelligent adjustable output force can be realized.

## 4. Magnetic Circuit Design

*4.1. Finite Element Model of Magnetic Circuit Structure.* The smart isolator improves the controllable range by using the magnetorheological effect of the MR material. The controllable performance of the MR material is limited by the magnetic circuit performance of magnetic field; therefore, the magnetic field analysis force of the isolator is essential. In this section, the magnetic field distribution characteristics of the MRE and MRG working plate are obtained by finite element simulation analysis, and it is proved that the arrangement of magnetic coils is feasible. In order to avoid the mutual interference between the upper and lower magnetic circuits, a magnetic insulating copper sheet was set in the middle position. The permeability of the insulating copper sheet is very small, which can hinder the passage of the magnetic circuit, thus reducing the mutual interference between the upper and lower magnetic circuits. Magnetic circuit design of the smart isolator can be shown in Figure 5.

Due to the symmetry of the magnetic circuit, three-dimensional electromagnetic field problem can be simplified into two-dimensional half axisymmetric planar electromagnetic fields. According to specific structure parameters of the isolator, the finite element model of the MRG and MRE cylinder can be established using plane 13 element of ANSYS, which is shown in Figure 6. A1 is 45# steel. A2 is MRG. A3 is the air. A4 is the excitation coil of the MRE working unit. A5 is the excitation coil of MRG working unit. A6 is the magnetic isolation material. A7 is MRE. The magnetic characteristic curve of MR material and steel is shown in Figure 7. The relative magnetic permeability of the magnetic isolation material and air is taken as 1. The simulation results of the smart isolator are shown in Figure 8.

*4.2. Magnetic Induction Curves.* Figures 9 and 10 show that how the magnetic induction varies with the current in the working channel of MRG and MRE cylinders of the smart isolator. The coil is wound around the magnetic material. The magnetic induction line passes through the middle of the magnetic material with coil entering current and spreads to the periphery in the way of the magnetic circuit, shown in Figure 5. In this process, the external magnetic line will spread outward; therefore, magnetic induction of the middle of working plates is the highest.

After MR materials preparation, structural design, and simulation analysis of the magnetic circuit, the MRG/MRE isolator was manufactured. The physical pictures of main parts and MRG/MRE isolator are shown in Figure 11.

## 5. Performance Testing of MRG/MRE Smart Isolator

To validate the rationality and feasibility of the designed smart isolator and investigate its performance, bi-directional universal testing machine (Model: CSS-283) in the Material Mechanics Laboratory of Mechanical Experimental Center of Hohai University was used to conduct performance testing. The experimental setup of the MRG/MRE isolator is presented in Figure 12. For the MRG/MRE isolator, tests were conducted using displacement control in the presence of sinusoidal mechanical excitation, and cases of test are horizontal shear displacement with current of 0 A, 1 A, and 2 A, respectively. Shear direction is shown in red arrows in Figure 12. The test is circulated 10 times for every case. Setting the maximum displacement at 6 mm for case of small displacement and at 12 mm for case of large displacement, it can be composed to 6 cases with test current, respectively, as 0 A, 1 A, and 2 A.

In the paper, high frequency refers to the case where small displacement is 6 mm while low frequency refers to the case where large displacement is 12 mm. Testing results of the MRG/MRE isolator are shown in Figure 13.

Table 3: The main design parameters of MRE smart isolator performance.

| | | | |
|---|---|---|---|
| Initial viscosity of MRG | 11.8 Pa·s | Initial shear modulus of MRE | 1.0 MPa |
| Yield strength of MRG | 92.1 kPa | Relative magnetorheological effect of MRE | 3 MPa |
| MRG consumption | 272 $cm^3$ | MRE consumption | 509 $cm^3$ |
| MRG working channel gap | 1 mm | Monolithic MRE thickness | 2 mm |
| Diameter of MRG working plate | 170 mm | External diameter of MRE working plate | 305 mm |
| Vertical pole diameter of working plate | 20 mm | Inner diameter of MRE working plate | 245 mm |
| Thickness of MRG cylinder | 15 mm | Thickness of MRE cylinder | 2 mm |
| Ultimate displacement of MRG working plate | 6 mm | Ultimate displacement of MRE working plate | 6 mm |
| Coil turns of MRG working plate | 1300 | Coil turns of MRE working plate | 1600 |
| Force range of small stroke | 3.63~9.30 kN | Force range of large stroke | 260.15~471.04 kN |
| Adjustable multiple of small stroke | 1.56 | Adjustable multiple of large stroke | 0.81 |
| Current range of MRG working plate | 0~2 A | Current range of MRE working plate | 0~2 A |
| Maximum power of MRG | <160 W | Maximum power of MRE | <200 W |
| | | Total height | 148 mm |

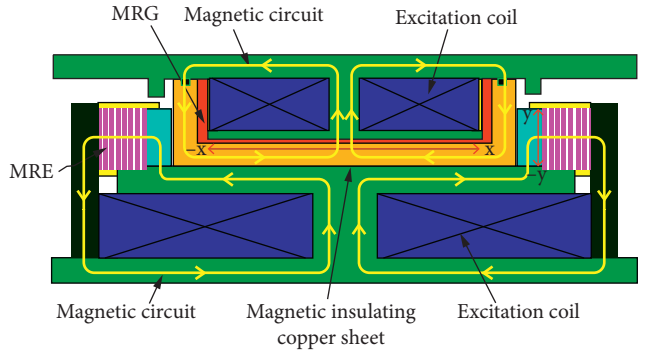


Figure 5: Magnetic circuit structure of the smart isolator.

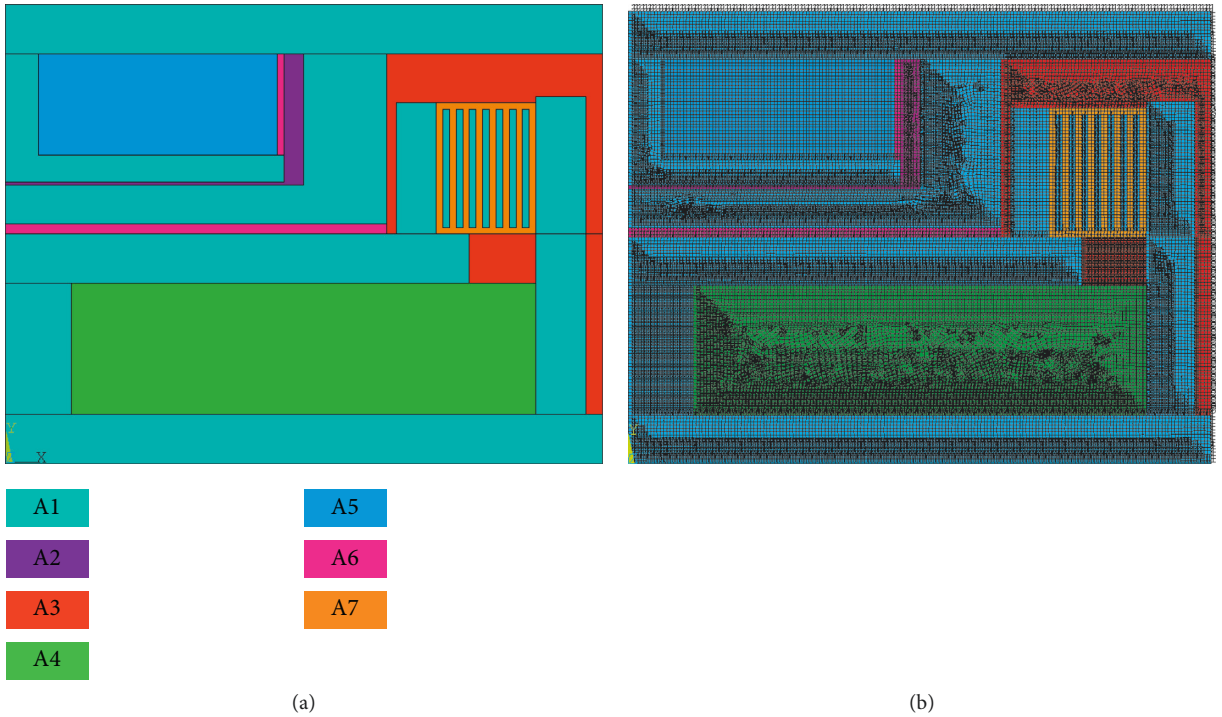


Figure 6: Finite element model of smart isolator. (a) Material partition. (b) Finite element meshing.

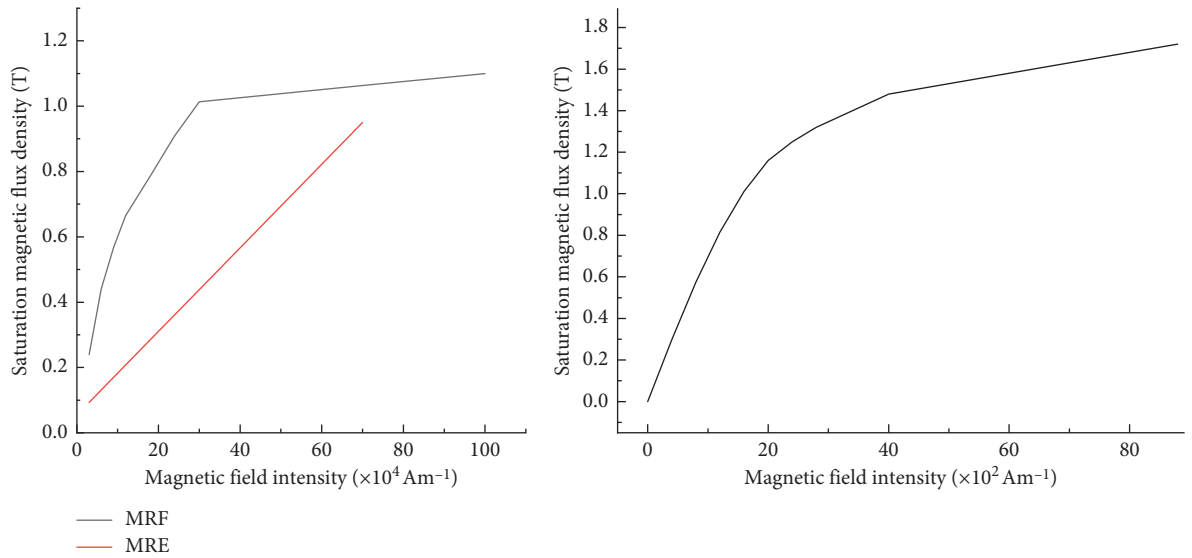


Figure 7: Magnetic characteristic curve of MR material and steel.

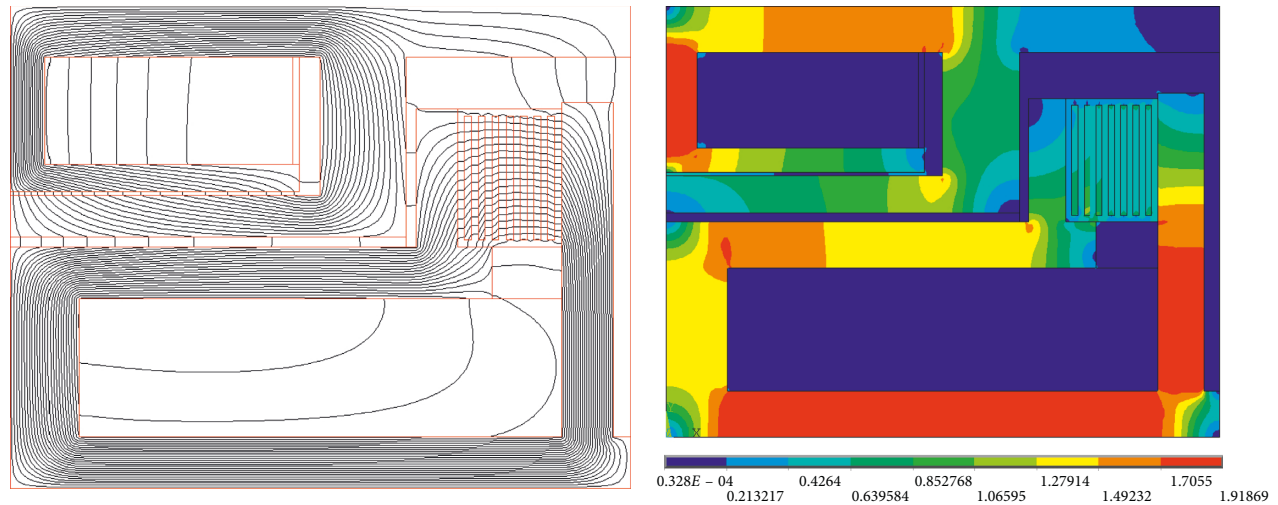


(a) (b)

Figure 8: The simulation results of the smart isolator. (a) Distribution of the magnetic flux lines. (b) Magnetic field density.

It can be seen from Figure 13 that maximum damping forces measured from the test agree well with the theoretical results shown in Table 3 and maximum output force of the isolator can meet the design requirements. The isolator has advantage of suppressing the displacement response. The damping force of the isolator can be adjusted in real time, which is suitable for structural vibration control.

Figure 13(a) shows the variation of force with small displacement ranging from −6 to 6 mm. It is MRG cylinder of the smart isolator that is suitable for the case of high frequency and small amplitude. It has characteristics of small damping, low dynamic stiffness, and high adjustable multiple. It also has the ability of shock resistance on high frequency, achieving design purpose of the isolator.

Figure 13 shows that the output range of the smart isolator is 3.5~10.6 kN with a small displacement of 6 mm and 198~429 kN with a large displacement of 12 mm. It is MRG cylinder and MRE cylinder of the smart isolator that work together and is suitable for the case of low frequency and large amplitude. It has characteristics of large damping and high dynamic stiffness, as well as the ability of vibration reduction on low frequency, achieving design purpose of the isolator. The smart isolator can be used in the engineering structure requiring earthquake resistance and vibration reduction with different output forces.

The capacity of energy dissipation and horizontal stiffness for the traditional isolator is not high, and the damping force-displacement curve only contains a narrow area with the small size. It can be seen from Figure 13(a)

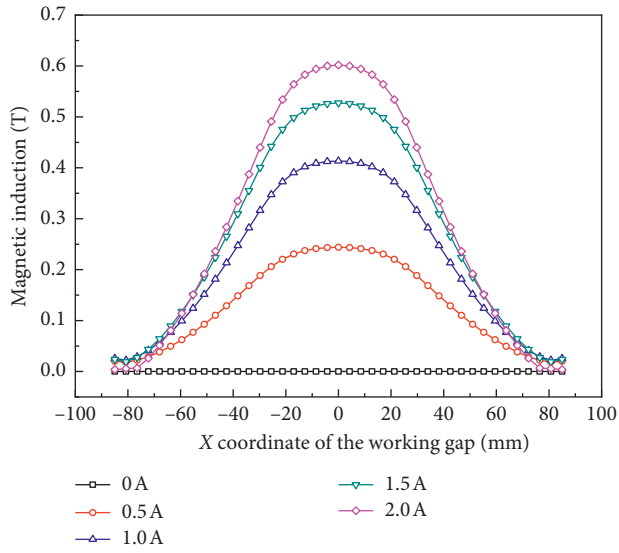


Figure 9: Magnetic induction curve in the working channel of the MRG cylinder.

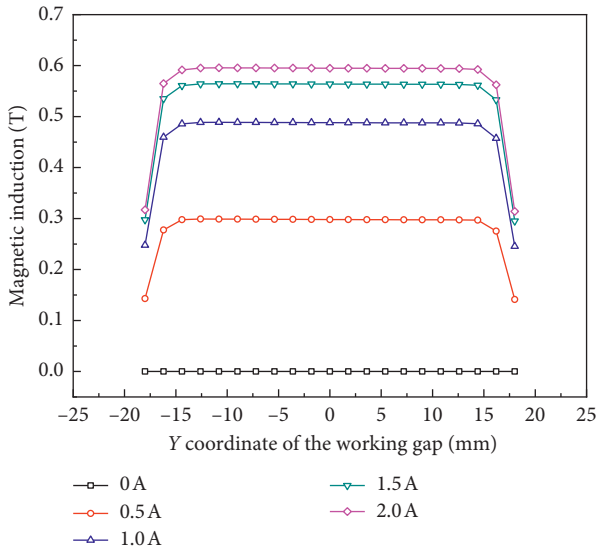


Figure 10: Magnetic induction curve in the working channel of the MRE cylinder.


Figure 11: Photographs of main parts and MRG/MRE isolator.

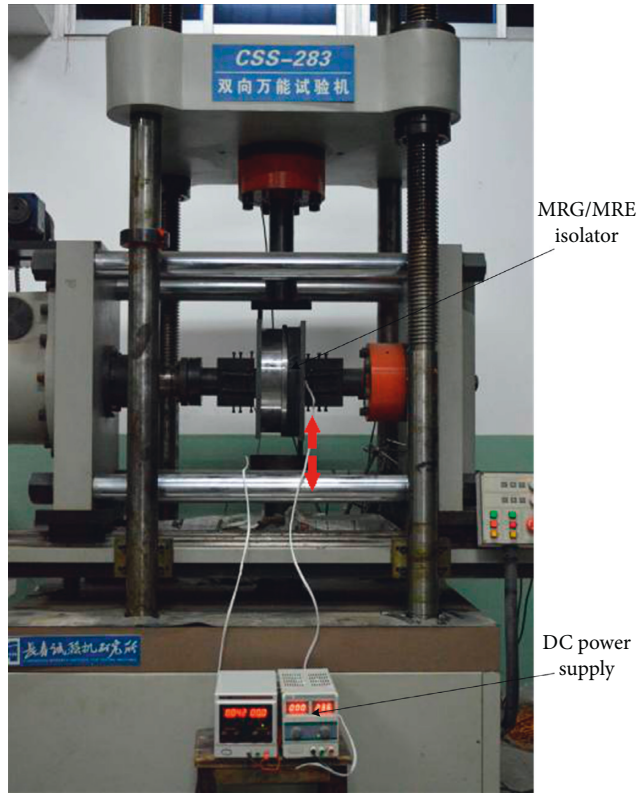


Figure 12: The experimental installation of the MRG/MRE isolator.

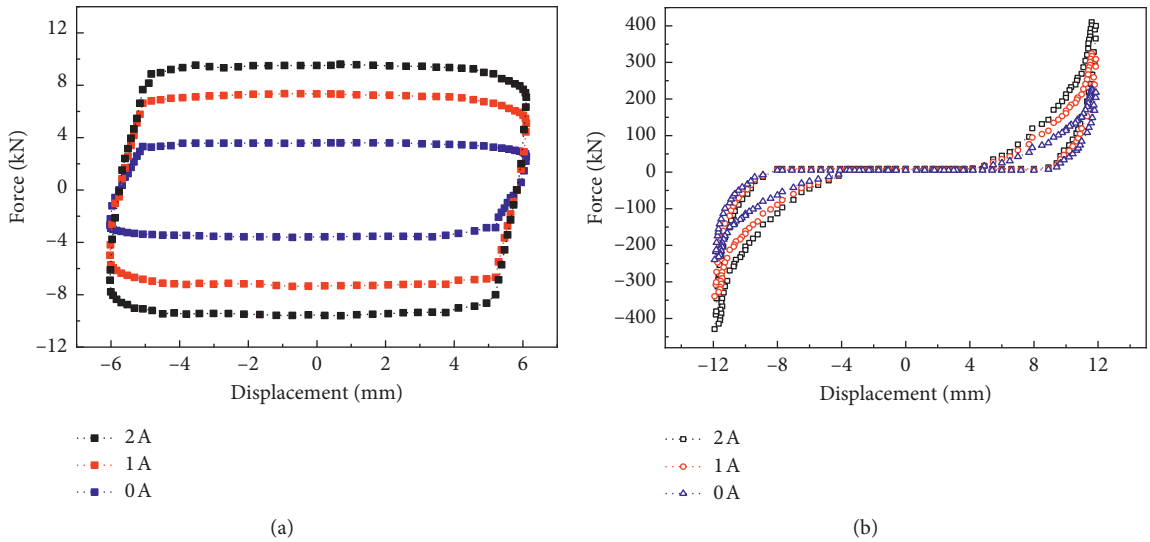


Figure 13: Load-displacement curve of the smart isolator. (a) Small displacement. (b) Large displacement.

that the damping force-displacement curve of the smart isolator in this project contains a large area which becomes bigger with increasing current and the hysteretic curve of the isolation device in large displacement from figure 13(b) includes that in small displacement from figure 13(a); hence, the smart isolator has a higher capacity of energy dissipation, and the performance of energy consumption will increase with the increasing current. Thus, the smart isolator designed in this study has better ability of energy dissipation.

## 6. Mechanical Model and Parameters Identification

*6.1. Mechanical Model of Smart Isolator Based on Uniaxial Model.* It is required to carry on the integral treatment on

the stiffness change point and the turning point when the dynamic analysis is carried out for various broken-line models. For models which require more consideration on multiaxis interaction or retaining stiffness and degradation, much processing is also needed for loading surface and yield mechanism (yield surface movement, changes of constitutive relationship, plastic flow, etc.). All of these require a lot of computing resources and are complex for use. These problems can effectively be solved using a nonlinear mechanical model suggested by Wen [24], in which a differential equation can be used to characterize the hysteretic characteristics of the isolator. For the isolator, equivalent restoring force model can be seen in Figure 14, where $k = \delta E A_r / T_r$ and $c = \eta A_p / h$, and the significance of the parameters in formulas is shown in Equations (2) and (3).

For the smart isolator designed in the paper, the restoring force of the nonlinear hysteretic system of the uniaxial model can be considered in two parts:

$$F(x, v) = \begin{cases} Av + (2/\pi) Bz(x, v), & a \le x \le b, \\ f(x) + h(v) + m(x), & x < a, x > b, \end{cases} \quad (5)$$

where $F(x, v)$ is the restoring force of the nonlinear hysteretic system of the isolator, which is a function of displacement $x$ and system velocity $v$; $Z(x, v) = \arctan(Ce^{Dv(t)+Ex(t)} - Ce^{-Dv(t)-Ex(t)})$; for small displacement, $v(t) = 6\cos(2\pi t/T), x(t) = 6\sin(2\pi t/T)$; $f(x) + h(v)$ is the restoring force of the nonhysteretic part, generally nonlinear, which is a function of velocity and displacement at a time; $m(x)$ is the restoring force of the hysteretic part; a and b equal to −6 mm and 6 mm for the designed isolator, respectively. $f(x) + h(v)$ can be seen as flexible resilience and viscous damping force, which is usually symmetrical in the process of loading and unloading, satisfies the symmetrical conditions. For example, it can be assumed as

$$\begin{aligned} f(x) &= b_0 \operatorname{sgn}(x) + b_1 x + b_2 x^2 \operatorname{sgn}(x) + b_3 x^3 + \cdots, \\ h(v) &= a_0 \operatorname{sgn}(v) + a_1 v + a_2 v^2 \operatorname{sgn}(v) + a_3 v^3 + \cdots, \\ \dot{m}(x) &= Hv - (\gamma \operatorname{sgn}(vm(x)) + \beta) |m(x)|^n v, \end{aligned} \quad (6)$$

where $H$, $\gamma$, $\beta$, and $n$ are the model parameters; parameter $H$ controls the amplitude of the hysteresis loop; $\gamma$ and $\beta$ control general shape of the hysteresis loop; $n$ controls the smoothness of the force-displacement curve. A variety of resilience models can be constructed such as stiffness hardening, degradation system, and narrowband or broadband system by adjusting the values of these parameters.

For the designed isolator, $H = 1$, $n = 1$, $\gamma = 0.25$, and $\beta = -0.75$. According to the test results of the intelligent isolator, its mechanical model can be built and parameters of the aforementioned formula and equation can be identified by using parameter identification. Identified parameters under different currents are shown in Table 4.

*6.2. Parameters Identification.* For parameters identification problem, the nonlinear least squares method is generally used, whereas the damping least square method is chosen in this study. The basic algorithm idea of the method is that to select the initial parameters and allowable error, then to calculate the objective function (sum of squared residuals) and observation matrix, and the correction value of the initial parameter can be obtained. Calculating the target function again based on new parameter and repeating after that, the parameter under the condition of the minimum objective function value can be obtained, which is the actual parameter value.

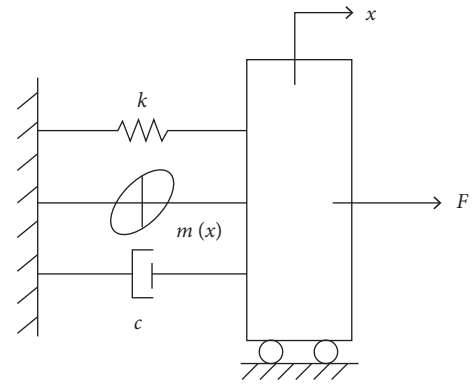


Figure 14: Restoring force model of the MRG/MRE isolator.

Table 4: Identified parameters under different current.

| I | A | B | C | D | E |
|---|---|---|---|---|---|
| 0 A | 0.1305 | 3.576 | −0.172 | 7.609 | −1.868 |
| 1 A | 0.2726 | −7.454 | 0.1721 | 7.608 | −1.867 |
| 2 A | 0.3563 | 9.698 | −0.1722 | 7.605 | −1.866 |

According to the aforementioned method, a set of data from the experiment of the isolation device in case of large displacement is selected and parameter of the mechanical model can be identified. We can obtain comparing diagram between the theoretical and experimental hysteresis curve of the isolator, as shown in Figure 15. Figure 15 shows theoretical results are in good agreement with the experimental results. Therefore, the parameter identification method can be regarded as a feasible and effective method.

## 7. Conclusion

In this paper, we designed and manufactured a MRG/MRE isolation device. Some key techniques of isolation damping device were addressed by conducting the performance tests. Rationality and correctness of smart isolator design have been verified based on the comparison of test measured and theory calculated result. Some conclusions can be drawn as follows:

(1) The MRG/MRE smart isolator structure designed in this study mainly includes MRG cylinder and MRE cylinder, which have resistance characteristic on high frequency and damping characteristic on low frequency, respectively. At small amplitude situation (6 mm), the designed isolator has characteristics of small damping and low dynamic stiffness that overcome stiffness hardening occurred on the traditional

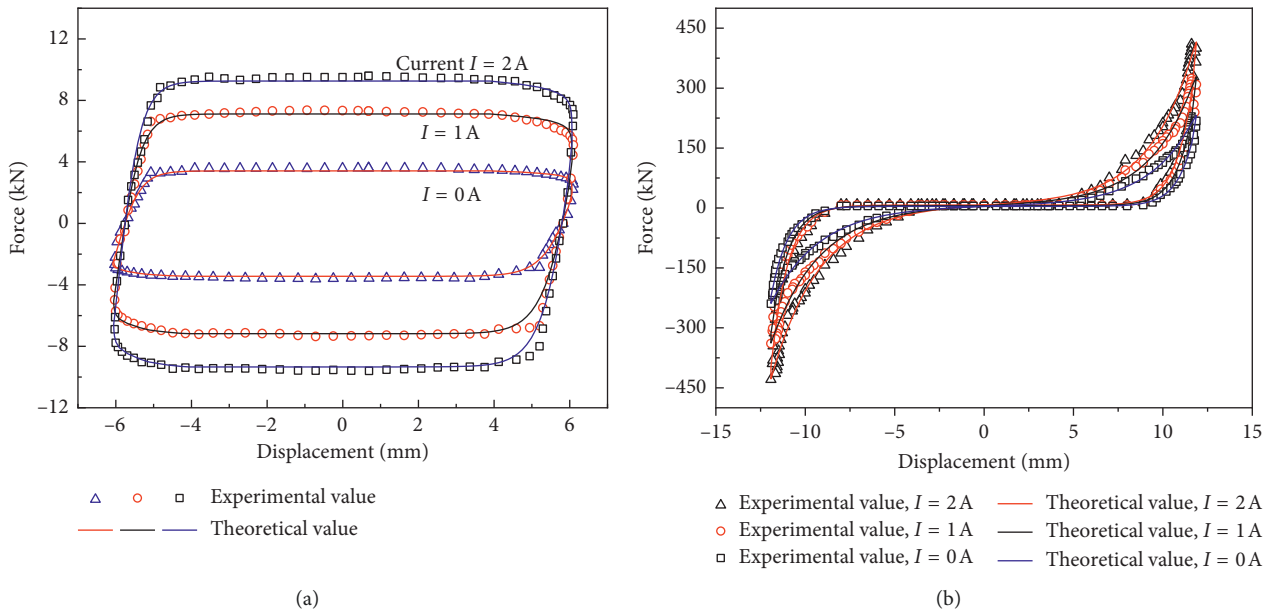


Figure 15: Comparison between theoretical and experimental results of the isolator. (a) Small displacement. (b) Large displacement.

isolator. While at large amplitude situation (12 mm), the isolator has characteristics of large damping and high dynamic stiffness that perform displacement control with larger damping force, which can be up to 429 kN.

(2) Model parameters of the smart isolator can be effectively identified using the least squares method based on the uniaxial mechanical model. The hysteresis curve of parameter simulation theoretically is in good agreement with the experimental results, which indicate that the method is feasible and effective.

(3) The key techniques developed in this study on structure, magnetic circuit, heat dispassion, and mechanical properties tests of the MRG/MRE isolator could provide a reference for smart isolation device with respect to reasonable parameter determination, design, and proper manufacturing. Usage of the designed MRG/MRE isolator can also provide a basis for the nonlinear vibration control design on actual civil building structures.

## Data Availability

The data used to support the findings of this study are available from the corresponding author upon request.

## Conflicts of Interest

The authors declare that there are no conflicts of interest regarding the publication of this paper.

## Acknowledgments

This work was supported by the National Natural Science Foundation of China (Grant no. 51508237), Primary Research and Development Plan of Jiangsu Province (Grant no. BE2017167), Natural Science Foundation of Jiangsu Province of China (Grant no. BK20140560), and the Research Foundation for Advanced Talents of Jiangsu University (Grant no. 14JDG161).

## References

[1] F. Guo, C. B. Du, G. J. Yu, and R. P. Li, "The static and dynamic mechanical properties of magnetorheological silly putty," *Advances in Materials Science and Engineering*, vol. 2016, Article ID 7079698, 11 pages, 2016.

[2] D. York, X. Wang, and F. Gordaninejad, "A new MR fluid-elastomer vibration isolator," *Journal of Intelligent Material Systems and Structures*, vol. 18, no. 12, pp. 1221–1225, 2016.

[3] C. Collette, G. Kroll, G. Saive, V. Guillemier, M. Avraam, and A. Preumont, "Isolation and damping properties of magnetorheologic elastomers," *Journal of Physics: Conference Series*, vol. 149, article 01209, 2009.

[4] Z. Xu, X. Gong, G. Liao, and X. Chen, "An active-damping-compensated magnetorheological elastomer adaptive tuned vibration absorber," *Journal of Intelligent Material Systems and Structures*, vol. 21, no. 10, pp. 1039–1047, 2010.

[5] S. Wang, W. Jiang, W. Jiang et al., "Multifunctional polymer composite with excellent shear stiffening performance and magnetorheological effect," *Journal of Materials Chemistry C*, vol. 2, no. 34, pp. 7133–7140, 2014.

[6] Y. Wang, S. Wang, C. Xu, S. Xuan, W. Jiang, and X. Gong, "Dynamic behavior of magnetically responsive shear-stiffening gel under high strain rate," *Composites Science and Technology*, vol. 127, pp. 169–176, 2016.

[7] X.-G. Lin, F. Guo, C.-B. Du, and G.-J. Yu, "The mechanical properties of a novel STMR damper based on magneto-rheological silly putty," *Advances in Materials Science and Engineering*, vol. 2018, Article ID 2681461, 15 pages, 2018.

[8] G. Yu, C. Du, and T. Sun, "Thermodynamic behaviors of a kind of self-decoupling magnetorheological damper," *Shock and Vibration*, vol. 2015, Article ID 502747, 9 pages, 2015.

[9] H. Kimura, S. Kondo, T. Ogawa et al., "Magneto-rheological grease composition," US20130123153A1 Patent, 2013.
[10] L. Chen, X. L. Gong, W. Q. Jiang, J. J. Yao, H. X. Deng, and W. H. Li, "Investigation on magnetorheological elastomers based on natural rubber," *Journal of Materials Science*, vol. 42, no. 14, pp. 5483–5489, 2007.
[11] M. Usman, S. H. Sung, D. D. Jang, H. J. Jung, and J. H. Koo, "Numerical investigation of smart base isolation system employing MR elastomer," *Journal of Physics: Conference Series*, vol. 149, article 012099, 2009.
[12] G. Liao, X. Gong, S. Xuan, C. Guo, and L. Zong, "Magnetic-field-induced normal force of magnetorheological elastomer under compression status," *Industrial & Engineering Chemistry Research*, vol. 51, no. 8, pp. 3322–3328, 2012.
[13] J. Fu, X. Zheng, M. Yu et al., "A new magnetorheological elastomer isolator in shear-compression mixed mode," in *Proceedings of 2013 IEEE/ASME International Conference on Advanced Intelligent Mechatronics*, Wollongong, Australia, July 2013.
[14] F. Jie, P. Li, G. Liao, J. Lai, and M. Yu, "Development and dynamic characterization of a mixed mode magneto-rheological elastomer isolator," *IEEE Transactions on Magnetics*, vol. 53, no. 1, pp. 1–4, 2016.
[15] N. Mohamad, S. A. Mazlan, Ubaidillah, S. B. Choi, and M. F. M. Nordin, "The field-dependent rheological properties of magnetorheological grease based on carbonyl-iron-particles," *Smart Materials and Structures*, vol. 25, no. 9, article 095043, 2016.
[16] H. An, S. J. Picken, and E. Mendes, "Nonlinear rheological study of magneto responsive soft gels," *Polymer*, vol. 53, no. 19, pp. 4164–4170, 2012.
[17] S. Sugiyama, T. Sakurai, and S. Morishita, "Vibration control of a structure using Magneto-Rheological grease damper," *Frontiers of Mechanical Engineering*, vol. 8, no. 3, pp. 261–267, 2013.
[18] T. Shiraishi and H. Misaki, "Vibration control by a shear type semi-active damper using magnetorheological grease," *Journal of Physics: Conference Series*, vol. 744, article 012012, 2016.
[19] S. S. Sun, J. Yang, W. H. Li et al., "Development of an isolator working with magnetorheological elastomers and fluids," *Mechanical Systems and Signal Processing*, vol. 83, pp. 371–384, 2017.
[20] S. Sun, J. Yang, W. Li, H. Deng, H. Du, and G. Alici, "Development of a novel variable stiffness and damping magnetorheological fluid damper," *Smart Materials and Structures*, vol. 24, no. 8, article 085021, 2015.
[21] C. Greiner-Petter, A. S. Tan, and T. Sattel, "A semi-active magnetorheological fluid mechanism with variable stiffness and damping," *Smart Materials and Structures*, vol. 23, no. 11, article 115008, 2014.
[22] M. R. Jolly, J. W. Bender, and J. D. Carlson, "Properties and applications of commercial magnetorheological fluids," *Journal of Intelligent Material Systems and Structures*, vol. 10, no. 1, pp. 5–13, 1998.
[23] X. Zhu, Y. Meng, and Y. Tian, "On mechanism of magnetic field induced compressive modulus of magnetorheological elastomers based on dipole Model," *China Mechanical Engineering*, vol. 21, no. 23, pp. 2861–2864, 2010.
[24] Y. K. Wen, "Method for random vibration of hysteretic systems," *Journal of Engineering Mechanics Divisions*, vol. 102, no. 2, pp. 249–263, 1976.